JJEES

Jordan Journal of Earth and Environmental Sciences

JJEES (2022) 13 (2): 89-96
ISSN 1995-6681

Kinematic and Q-slope Application for Stability Assessment of the Rock Slopes Along Goshan_Qupy Qaradagh Road, Sulaimaniyah, NE-Iraq

Ghafor Ameen Hamasur

Department of Geology, College of Science, University of Sulaimani, Sulaimaniyah, Iraq

Received 5 July 2021; Accepted 4 September 2021

Abstract

In the mountainous areas of Iraqi Kurdistan, road and highway networks play a significant role in far-away transportation and social activities. Any slope failure may lead to traffic disruption, and loss of lives. The undesigned excavations of rock slopes for construction or expanding purposes may weaken the slope stability.

In this study, eight (8) cut-rock slope stations have been chosen along Goshan–Qupy Qaradagh tourist road at Sulaimani, NE-Iraq, and these are for evaluating the stability of cut-rock slopes by various techniques. The choice of slope stations was based on variation in the discontinuities pattern, slope morphology, and type of failure. The field data were analyzed for their possible degree of stability by slope kinematic analysis, using DIPS v6.008 software, and to examine the stability condition, the Q-slope system, which is a practical way for rock slope engineering classification, was also used.

Slope kinematic analysis revealed three types of failures, i.e., Planar sliding, wedge sliding, and direct toppling failure. Planar sliding may occur in rock slopes of stations 1, 2, 4, and 8, wedge sliding in rock slopes of stations 3, 4, and 6, direct toppling in rock slope of station 7, and no failures may occur in the rock slope of station 5.

The results of Q-slope revealed that the rock slopes in stations 1, 2, 3, 4, 6, 7, and 8 are in unstable condition, whereas the rock slope in station 5 is in stable condition.

Keywords: *Slope stability, Kinematic analysis, Q-slope system, High-folded zone, Western Zagros, Northeast Iraq.*

1. Introduction

Many researchers such as Basahel and Mitri (2017), Sarannathan and Kannan (2017), Sharma et al., (2019), studied the rock slope stability along with road cuts that are joining far-away areas in the valleys-plains and mountain slopes. Also, there are many engineering geological studies about "rock slope stability" in Iraq such as those that used the kinematic method (Mamlesi, 2010), other study used the landslide possibility index (LPI) method (Hamasur, 2013), also several studies were used kinematic method and slope mass rating (SMR) system (Hussien et al., 2020; Hamasur & Qadir, 2020),

There are many engineering classification systems, some have been developed for specific purposes like slope engineering design and some have been developed for general assessments (Azarafza et al., 2017). The engineering classification systems were developed practically by determining the essential parameters, yielding each parameter a digital value and a rating factor. This is made, via empirical formulae, to determine the final value for a rock mass. The final value has a relation to the underground excavation stability, which is used for the evolution of the engineering classification system (Hack et al., 2003).

There is no stability evaluation of the rock slopes by the Q-slope system in Iraq and the Iraqi Kurdistan region, so this study is the first one that is done with the mentioned system.

In this study, slope kinematic analysis and the Q-slope system are utilized to assess the stability of cut-rock slopes along Goshan – Qupy Qaradagh road.

The study area is located about 36 km (aerial distance) to the southwest of Sulaimaniyah, city-NE Iraq, and along Goshan – Qupy Qaradagh road, between latitudes 35° 15′ 58″ N - 35° 16′ 50″ N and longitudes 45° 21′ 09″ E - 45° 22′ 53″ E, (Figure 1).

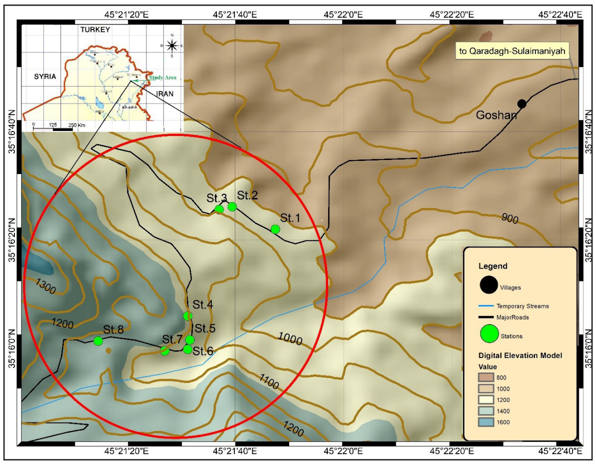

Figure 1. Topographic map showing the location of the study area

* Corresponding author e-mail: ghafor.hamasur@univsul.edu.iq

2. Geological setting

From the tectonic point of view, the area is located in the western Zagros fold-thrust belt's high-folded zone. Structurally, the area shows a homoclinal structure that dips towards the northeast at an intermediate - high dip angle, whereas a homocline is a structure where the sequence layers of rock strata, dip uniformly in one direction, that has approximately the same inclination (Jackson et al., 2005; Huggett, 2011). A homocline can be combined with limbs of a dissected fold (Bloom, 1998; Gerrard, 1998), in the area of study, the homoclines that are existed in Fat'ha (Lower Fars), Pilaspi, and Sinjar Formations run with the NE-limb of Sagrma anticline.

Geomorphological landforms in the study area are depositional, erosional, and structural landforms.

The most conspicuous landforms in the selected slope stations for stability study represent homoclinal ridges. Homoclinal ridges are the expression of dipping strata, typically sedimentary strata, that consist of alternating beds of hard and weak strata (Twidale and Campbell, 1993), in the study area, the detrital limestone of Fat'ha (Lower Fars) Formation, limestone of Pilaspi and Sinjar Formations represent the hard resistant strata, the red claystone and siltstone of Fat'ha Formation, marl of Pilaspi Formation and marl with shale of Sinjar Formation represent the weak non-resistant strata.

Stratigraphically the study area was composed from old to young of Sinjar, Gercus, Pilaspi, and Fat'ha Formations (Figure 2) (Abdullah and Qayim, 2016). Sinjar Formation consists of intermediate-massive beds of detrital and fossiliferous limestone that are intercalated with marl beds. Gercus Formation consists of a red clastic sequence of pinkish red to purple siltstone and claystone alternating with gray to reddish-brown coarse-grained sandstone, and occasionally the conglomerate bed may exist at the bottom of sandstone beds. Pila Spi Formation consists of well-bedded, highly fractured limestone, dolomitic limestone, dolomite, chalky limestone, and Fat'ha Formation alternating sedimentary cycles of yellowish-gray fossiliferous limestone, green marlstone, claystone, siltstone, and sandstone.

The cut-rock slopes are composed of thin-intermediate beds of detrital (stations 1and 2), detrital limestone with a succession of marl and intercalation of sandstone beds (station 3), thick conglomerate beds in the upper part, and claystone in the lower part (station 4), thin-thick beds of limestone and dolomitic limestone (stations 5, 6 and 7) and intermediate-massive beds of detrital and fossiliferous limestone that are intercalated with marl beds (station 8). The cut-rock slopes have steep to very steep dip angles with a developed discontinuities system (Table 1).

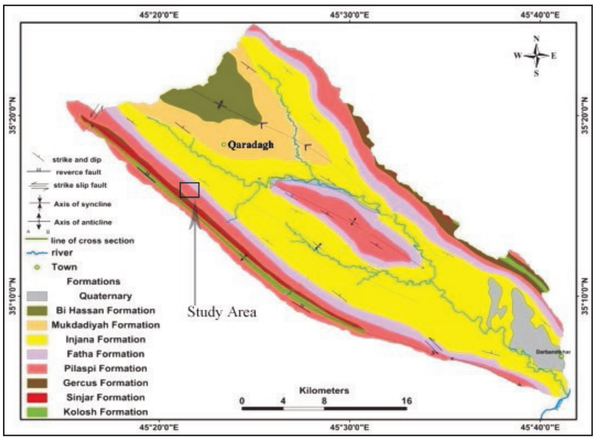

Figure 2. Regional geological map showing the location of the study area (Abdullah and Qayim, 2016)

Table 1. Dip direction /Dip angle of slope face, bedding, and joint sets at the stations (rock slopes) of the area under study.

Station No. (Slope site)	Geologic Formation	Slope (Direction / Angle)	Bedding plane Dip direction / Dip	Join set (J1) Dip direction / Dip	Joint set (J2) Dip direction / Dip	Joint set (J3) Dip direction / Dip	Joint friction Angle (ϕ)
1	Fat'ha (Lower Fars)	035°/60°	048°/41°	324°/88°	223°/60°	--------	21°
2		045°/80°	052°/42°	321°/88°	235°/47°	--------	21°
3		255°/80°	049°/44°	322°/70°	234°/50°	--------	36°
4	Contact of Fat'ha / Pilaspi	070°/70°	052°/50°	170°/72°	265°/40°	307°/71°	36°
5	Pilaspi	122°/80°	050°/60°	320°/86°	230°/28°	--------	36°
6		130°/80°	050°/60°	140°/75°	231°/35°	-------	36°
7		212°/70°	050°/62°	310°/67°	225°/30°	-------	36°
8	Sinjar	165°/65°	050°/60°	148°/57°	315°/70°	-------	36°

3. Methodology

3.1. General Methodology

In tunneling and underground mining, the following empirical engineering systems are used to give appropriate support and reinforcement for specific excavation spans:

* Q-system (Barton et al., 1974)

* Rock mass rating (RMR) (Bieniawski, 1976; Bieniawski, 1989).

For rock slope stability, engineering systems are less used, and either easy kinematics or numerical modeling may be chosen. The following empirical engineering systems were developed to predict the support, reinforcement, and performance of excavated slopes (Bar and Barton, 2017).

* SMR: slope mass rating (Romana, 1985).

* Global slope performance index (Sullivan, 2013).

None of the mentioned previous rock engineering systems supply guidance concerning appropriate, long-term stable slope angles in which rock reinforcement and support are absent (Bar and Barton, 2017).

3.2. Methods in the study area

Detailed engineering geological survey was carried out at eight (8) cut-rock slope stations, three (3) of them (stations No. 1, 2 & 3) are in Ft'ha Formation, station No.4 is at the contact of Fat'ha / Pila Spi Formations, Stations No.5, 6 & 7 are in Pila Spi Formation, and station No.8 is in Sinjar Formation. All field attitude measurements of discontinuities (bedding planes and joints) and results are in the dip direction/dip amount manner.

The assessment of rock slopes hints at qualitative and quantitative assessments for different rock mass components. This study concentrates on the stability evaluation of the cut-rock slopes by kinematic analysis and the Q-slope system.

Slope kinematic analysis is the easy failure analysis in terms of joint sets, bedding plane, slope, and sliding friction angle, it is only practical for preliminary design (Hoek and Bray, 1981). The kinematic analysis is a way of determining the probable failure types (plane, wedge & toppling) in jointed rock mass from the relation between discontinuities and slope surface (Hoek and Bray, 1981). Markland test (Markland, 1972) is a method designated to evaluate the probability of wedge sliding. In contrast, the wedge-shaped mass slides along the intersection line of two geological planes, the planar sliding may occur when a discontinuity dips in the same direction (within 20°) as the slope face, at an angle less than the angle of the slope but larger than the friction angle along the sliding surface. A satisfactory improvement to Markland's test has been made as Hocking (1976), and the flexural toppling failure may occur when a sharply dipping discontinuity is parallel or subparallel to the slope face (within 30°) and dips into it (Goodman, 1989), Block toppling (direct and oblique toppling) requires the converging of two discontinuities to create detached blocks. Furthermore, the presence of the basal plane facilitates the occurrence of block toppling. The field data were analyzed stereographically using DIPS v6.008 software (Rocscience, 2015). Friction angles of potential failure planes were calculated by the tilting method (Bruce et al., 1989).

Q-slope is a practical engineering system that allows the quick assessment of the stability of natural cut, artificially cut-rock slopes, roads, and cuttings of the railway in the field, during or after excavation. This system is based on the perception and utilized as a first assessment in the field stage (Barton and Bar, 2015).

Q-slope is modified from the Q-system, which has been used for the rock exposure characterization, core, and tunnels (Barton et al., 1974; Barton and Grimstad, 2014).

During excavation, the Q-slope use reduces the support requirements or bench-width needs (in larger slope profiles) of slopes that permit geotechnical engineers to evaluate in-situ excavated rock slope stability and make slope angle adjustments as the condition of the rock mass evident during construction. In 2015, tests on several engineering projects worldwide have revealed a straightforward correlation between Q-slope values and unsupported stable slope angles for a long time (Barton and bar, 2015).

Barton and Bar (2015) recommend that it can be used for all types of rock slope failures such as planar, wedge, toppling, and local debris failures.

Q-slope uses the same six parameters RQD, Jn, Jr, Ja, Jw, and SRF of standard Q-system. The Q parameters (RQD, Jn, Jr, and Ja) remain unaltered in the Q-slope system, and a new way for estimating Jr/Ja ratios for the two sides of probable wedges may be utilized along with applying orientation factors. Jw, who is now termed J_{wice}, considers a broader range of environmental conditions agree with rock slopes, which acted for a long time. These conditions include severe erosive rainfall and ice effects, as may seasonally occur at opposite ends of the rock type. There are also slope-relevant SRF (SRF_a, SRF_b, and SRF_c) categories (Barton and Bar, 2015; Bar and Barton, 2016; Bar and Barton, 2017). Q-slope is determined using the expression after (Barton and Bar, 2015):

$$\text{Q-slope} = (RQD / J_n) \cdot (J_r / J_a)_o \cdot (J_{wice} / SRF_{slope}) \quad .... (1)$$

Where: RQD= Rock Quality Designation.

J_n = Joint set number.

J_r = Joint roughness number.

J_a = Joint alteration number.

O =Orientation factor.

J_{wice} = Condition Number of environment and geology.

SRF_{slope} = Strength Reduction-Factor related to the slope.

SRF_a = SRF is related to Physical condition.

SRF_b = SRF is related to stress.

SRF_c = SRF is related to major discontinuity.

Barton and Bar (2015) proposed a simple formula for the steepest slope angle (β) not needing reinforcement or support for slope heights less than 30 m. This formula is now extended to all slope heights (Bar and Barton, 2017):

$$\beta = 20 \log_{10} \text{Q-slope} + 65^{\circ} \quad .... (2)$$

Equation 2 matches the slopes ranged between 35° and 85°.

4. Results and Discussion

The cut-rock slopes create the best places for determining the lithological variations, weathering conditions, and the outcrops' structural geological behaviors to record discontinuity patterns. This study comprised an investigation of slopes at eight (8) stations (cut-rock slope sites) with different geotechnical characteristics.

The cut-rock slopes have steep to very steep dip angles with a developed discontinuities system, as in Table 1.

Kinematic analysis of cut-rock slopes was achieved for failure controlled by structure, utilizing DIPS v6.008 software (Rocscience, 2015). The kinematic analysis results reveal the probability of planar sliding in stations 1, 2, 4, and 8 (Figures 3, 4, 6, and 10). The probability of wedge sliding in stations 3, 4, and 6 (Figures 5, 6, and 8). Only station No.7 shows the probability of direct toppling (Figure 9). Also, kinematic analysis reveals that the slope in station 5 is stable (Figure 7).

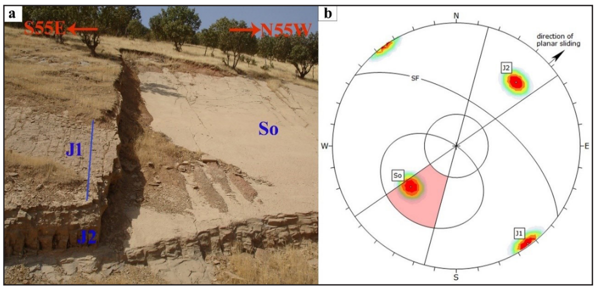

Figure 3. a-Field view for station No.1 with marked discontinuity sets. b-Kinematic analysis for station No.1 shows planar sliding on the bedding plane (So). Where: SF=slope face; J1= joint set No.1; J2= joint set No.2, the pink color is a possible failure zone

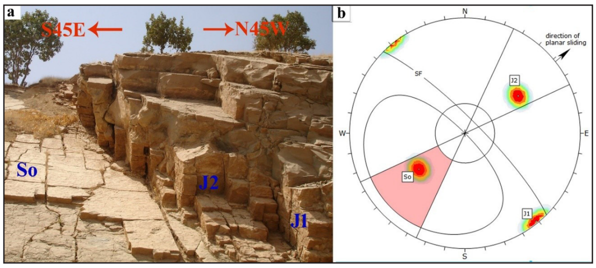

Figure 4. a-Field view for station No.2 with marked discontinuity sets. b-Kinematic analysis for station No.2 shows planar sliding on the bedding plane (So)

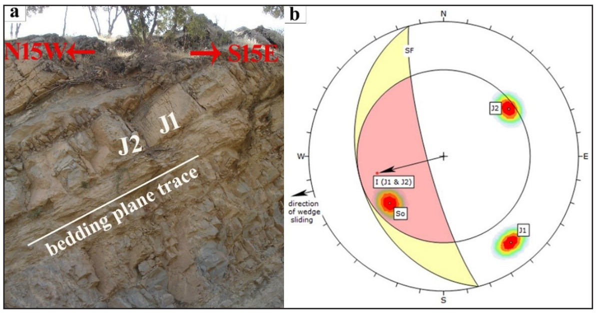

Figure 5. a-Field view for station No.3 with marked discontinuity sets. b-Kinematic analysis for station No.3 shows wedge sliding on J1 and J2. Where: I=intersection between two discontinuity sets

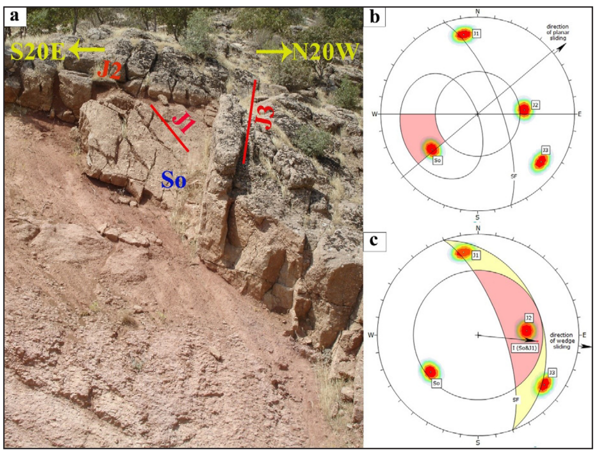

Figure 6. a-Field view for station No.4 with marked discontinuity sets. b-Kinematic analysis for station No.4 shows planar sliding on the bedding plane (So). c-Wedge sliding on So and J1

All cut-rock slope stations are sites that already failed (Figures 2(a), 4(a), 5(a), 6(a), 7(a), 8(a), 9(a) and 10(a)). The results of kinematic analysis in all stations are listed in Table 2.

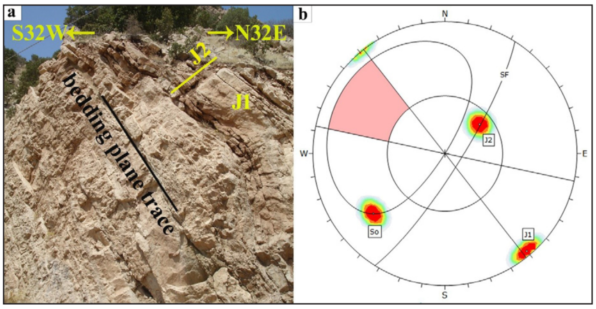

Figure 7. a-Field view for station No.5 with marked discontinuity sets. b-Kinematic analysis for station No.5 shows that the slope is stable

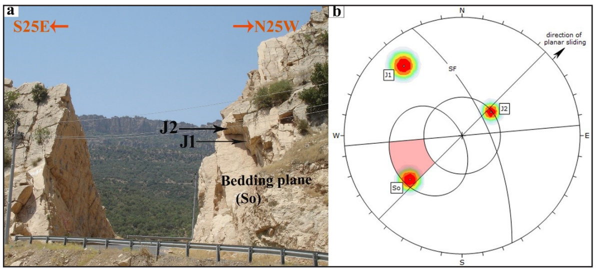

Figure 8. a-Field view for station No.6 with marked discontinuity sets. b-Kinematic analysis for station No.6 shows planar sliding on the bedding plane (So)

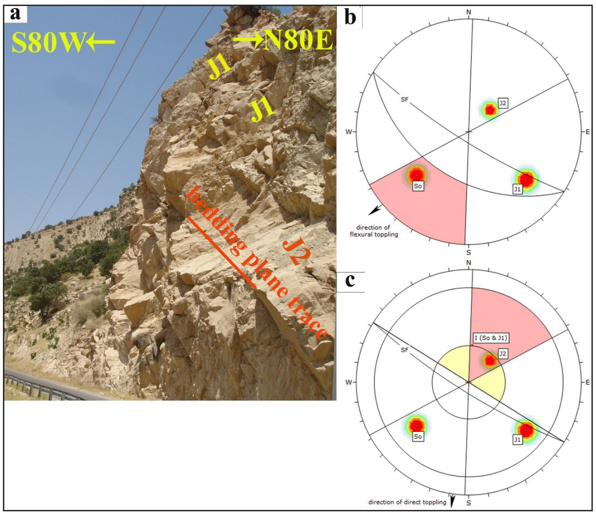

Figure 9. a-Field view for station No.7 with marked discontinuity sets. b-Kinematic analysis for station No.7 shows flexural toppling about So. c- Direct toppling via release intersected planes (So & J1)

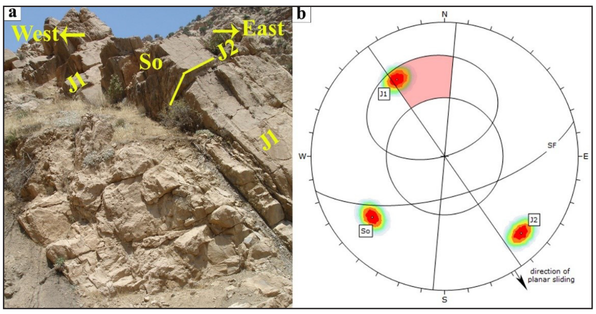

Figure 10. a-Field view for station No.8 with marked discontinuity sets. b-Kinematic analysis for station No.8 shows planar sliding on the J1

Table 2. Results of kinematic analysis in all slope stations, using DIPS-Software.

Station No. (Slope site)	Planar sliding & its direction	Wedge sliding & its direction	Flexural toppling & its direction	Direct toppling & its direction
1	√ (048°)	--------	--------	--------
2	√ (052°)	--------	--------	--------
3	--------	√ (255°)	--------	--------
4	√ (052°)	√ (096°)	--------	--------
5	--------	-------	--------	--------
6	√ (050°)	--------	--------	--------
7	--------	--------	√ (230°)	√ (187°)
8	√ (148°)	--------	--------	--------

The six mentioned parameters calculated Q-slope values for the eight cut-rock slopes. Palmstrom-way was utilized in the estimation of the average spacing and frequency of discontinuities sets, also estimating the volumetric joint count, and then calculating RQD-value from the relation of RQD with joint counting in a unit volume (Jv) (RQD = 110 -2.5 Jv) (Palmstrom, 2005), as shown in Tables 3 and 4.

Table 3. Joints count in a unit volume (Jv), Rock-Quality Designation (RQD), and average spacing of all discontinuities observed in the detrital limestone of Fatʾha (Lower Fars) Formation at station No.1.

Discontinuities (Bedding plane and Joints)	Set spacing and frequency				Average spacing(m)	Average frequency*
	Spacing (m)		Max. frequency	Min. frequency		
	Min.	Max.				
Bedding plane (S_o)	0.10	0.40	10	2.5	0.25	4
Joint set 1 (J_1)	0.30	4	3.333	0.25	2.15	0.465
Joint set 2 (J_2)	0.2	3	5	0.333	1.60	0.625
2Random joint **						
Volumetric joint count Jv=∑Frequencies (joints/m^3)						5.09
RQD = 110 – 2.5 Jv……………. (RQD=100 for Jv ≤ 4)					97	

Table 4. Joints count in a unit volume (Jv), Rock-Quality Designation (RQD), and average spacing of all discontinuities observed in all stations.

Geologic Formation	Lithology	Station No.	Jv (joints /m^3)	RQD
Fatʾha (Lower Fars)	Detrital Limestone	1	5.09	97
	Detrital Limestone	2	5.803	95
	Detrital Limestone	3	5.261	96
Contact of Fatʾha/Pilaspi	Basal Conglomerate	4	3.479	100
Pilaspi	Limestone	5	4.395	99
	Limestone	6	2.483	100
	Limestone	7	2.483	100
Sinjar	Limestone	8	4.741	98

Uniaxial compressive strength (UCS) of intact rock was estimated indirectly from the point load test, utilizing the procedure of ISRM (1985), with an index-to-strength conversion factor equal to 21 (k=21), this value seems to be working well for a variety of rock types (Rusnak and Mark, 2000). The results of the mentioned test have appeared in Table 5; UCS-value in conjunction with maximum principal stress (б1) is necessary for estimating the SRF_b - stress. The climatic condition of the study area is semi-arid (six months are very rainy and cold, whereas the other six months are dry and semi-hot to hot), and because most landslides have occurred during rainy seasons, so the environmental condition is considered as a a wet environment for J_{wice}. The summary of the rock mass's characterization for the Q-slope parameters in the mentioned cut-rock slope stations has appeared in Table 6. After determining the rock mass characteristics in each rock slope station, the required Q-slope parameters were rated from a comparison of parameters characteristic (Table 6) with standard Q-slope Tables of Barton and Bar (2015).

Table 5. Results of the Point-load test and value of uniaxial compressive strength (UCS) of the intact rock in the rock slopes of stations 1, 2, 3, 4, 5, 6, 7 & 8.

Station. No	1	2	3	4	5	6	7	8
Geologic Formation	Fat'ha (Lower Fars)			Contact Fat./Pila.	Pila Spi			Sinjar
D (mm)	45	40	45	42	40	45	50	40
W (mm)	50	52	46	60	50	45	55	60
F (KN)	5.1	6.86	5.6	6.84	12.2	12	15	13.1
F (MN)	0.0051	0.00686	0.0056	0.00684	0.0122	0.012	0.015	0.0131
A (mm^2)	2250	2080	2070	2520	2000	2025	2750	2400
$D_e^2=(4A/\pi)$ m^2	0.00286	0.00264	0.00263	0.0032	0.00254	0.00257	0.00349	0.00305
$Is=F/D_e^2$ (MPa)	1.78321	2.59848	2.12927	2.1375	4.80314	4.66926	4.29799	4.29508
$f=(D/50)^{0.45}$	0.95369	0.90446	0.95369	0.92453	0.90446	0.95369	1	0.90446
$Is_{(50)}=Is*f$	1.70062	2.35022	2.03066	1.97618	4.34424	4.45302	4.29799	3.88472
$UCS=21*Is_{(50)}$ (MPa)	35.713	49.354	42.643	41.5	91.229	93.513	90.257	81.579
UCS (MPa)	36	49	43	42	91	94	90	82

Where: D=Diameter (distance between the two loaded points), W=Width of the specimen
A=W*D((Area of idealized failure plane), F=Force at failure,Is=Point load strength index
f =(size correction factor), UCS=uniaxial compressive strength.

Table 6. Characterization of the rock mass for the Q-slope parameters in all slope stations.

Formation	Fatha (Lower Fars)			Contact Fat./Pila.	Pila Spi			Sinjar	Remarks
Slope Station	1	2	3	4	5	6	7	8	
Slope Height(m)	16	10	10	10	10	20	70	10	From field
б$_1$ (MPa)	≈ 0.4	≈ 0.25	≈ 0.25	≈ 0.25	≈ 0.25	≈ 0.5	≈ 1.75	≈ 0.25	б$_1$=Ɣ. h
UCS (=бc) (Mpa)	36	49	43	42	91	94	90	82	Table 5
бc / б1	90	196	172	168	364	188	51	328	
Failure Mode	Planar sliding	Planar sliding	Wedge sliding	* PS *WS	Stable slope	Planar sliding	Direct toppling	Planar sliding	Table 2
RQD	97	95	96	100	99	100	100	98	Table 4
Jn	F	F	F	G	F	F	G	H	
Jr	C	C	C	C	C	F	F	C	
Ja	OPR	OPR	E	E	C	B	B	E	
O-Factor	A- Causing failure if unsupported.	A- Causing failure if unsupported	A-VUnfa B- VUnfa	*PS:VUnfa. *WS:VUnfa B-Fav.	A- Very favorably oriented	A-Very Unfa.	A- Causing failure if unsupported	A- Causing failure if unsupported	
J wice	Un-Com WE	Un-Com WE	Un-Com DE+WE	Un-Com WE	St-Com WE	Un-Com WE	Un-Com WE	Un-Com WE	
SRF_a	B	B	B	B	A	A	B	B	
SRF_b	F	F	F	F	F	F	F	F	
SRF_c	L (very unfav.)	L (very unfav.)	L (very unfav.)	L(PS:Vunf WS: Unfa.	L (fav.)	L (fav.)	L (unfav)	L (very unfav)	

Where: б1=Maximum principal stress (Ɣ-rock ≈ 0.025MN/m^3), Fat.=Fatha, Pila.=Pila SpiUCS (бc)=Uniaxial compressive strength,PS=Planar sliding, WS=Wedge sliding,
(For Jn: F=Three joint sets, G=Three joint sets plus random joints, H=Four or more joint sets)
(For Jr: C=Smooth, undulating; F=Smooth, planar)
(For Ja: OPR=Thick, continuous zones or bands of clay; B=Unaltered joint walls, surface staining only; C=Slightly altered joint walls. Non-softening mineral coatings, sandy particles, clay-free disintegrated rock, etc; E=Softening or low friction clay mineral coatings, i.e., kaolinite or mica. Also chlorite, talc, gypsum, graphite, etc., and small quantities of swelling clays)
(For SRF_a: A=Slight loosening due to surface location; B=Loose blocks, signs of tension cracks and joint shearing, susceptibility to weathering)
(For SRF_b: F= Moderate stress-strength range (σ_c/σ_1: 50-200 or greater))
VUnfa.=Very Unfavorable,Fav.=Favorable, Unfa.=Unfavorable,
Un-Com=Unstable structure-Competent rock, St-Com=Stable structure-Competent rock,
WE=Wet Environment, L=Major discontinuity with little or no clay

Finally, the Q-slope values were determined for rock slopes in each station, as shown in Table 7.

Table 7. Rating of the Q-slope parameters, Q-slope value, slope angle and stable slope angle.

Formation	Lower Fars (Fatha)				Pila Spi			Sinjar	Remarks
Slope Station	1	2	3	4	5	6	7	8	
RQD	97	95	96	100	99	100	100	98	Table 4
Jn	9	9	9	12	9	9	12	15	From Compar-ison of Table 6 with standard Q-slope Tables
Jr	2	2	2	2	2	1	1	2	
Ja	10	10	4	4	2	1	1	4	
O-Factor	0.25	0.25	A=0.5 B=0.8	PS: 0.5 WS:A-0.5 B-0.9	2	0.5	0.25	0.25	
J wice	0.6	0.6	0.6	0.6	0.7	0.6	0.6	0.6	
SRF_a	5	5	5	5	2.5	2.5	5	5	
SRF_b	2.0	1.5	1.5	1.5	1	1.5	2.0	1	
SRF_c	8	8	8	PS: 4 WS: 2	1	1.5	8	8	
Max. SRF	8	8	8	PS: 5 WS: 5	2.5	2.5	8	8	
Qslpoe-value	0.0404	0.0395	0.08	PS;0.25 WS:0.1125	6.16	1.33	0.1562	0.0612	
Slope angle	60	80	80	70	80	80	90	65	Table 1
Stability cond-ition of slope	Unsta-ble	Unsta-ble	Unsta-ble	Unsta-ble	Stable	Unsta-ble	Unsta-ble	Unsta-ble	Fig. 11
Stable slope angle without support	≈ 37	≈ 37	≈ 43	PS: ≈ 53 WS: ≈ 46	≈ 81	≈ 68	≈ 49	≈ 41	Equation No. 2
Where: PS=Planar sliding, WS=Wedge sliding									

To determine the stability condition of cut-rock slopes in each station, the Q-slope value and slope dip angle in each station were projected on the Q-slope chart. The location of this projection on the chart defines the slope stability condition (Figure 11). Figure 11 reveals that the cut-rock slopes are unstable in stations 1, 2, 3, 4, 6, 7, and 8, and the cut-rock slope is stable in station 5. Also, the sharper slope angle (β) not needing support or reinforcement was determined from formula number 2 (Table 7).

Q-slope system reveals that the slopes with the same slope angle are more stable with increasing Q-slope value, this relation is obvious from a comparison among slope stations 2, 3, 6 and 5. whereas the slope with the same Q-slope value are more stable with decreasing the slope angle and they are stable in the same slope angle, this relation is obvious from the comparison between slope stations 1 and 2 (Figure 11).

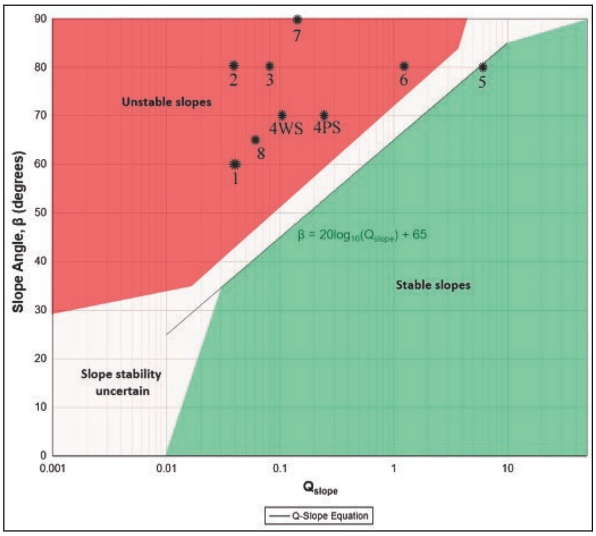

Figure 11. Stability condition of cut-rock slopes in the studied stations, where: PS=Planar sliding; WS=Wedge sliding

5. Conclusions

The Slope kinematic analysis revealed four types of failures, i.e., Planar sliding, wedge sliding, flexural toppling, and direct toppling failures.

The Q-slope results revealed that the rock slopes in seven stations are unstable, whereas the rock slope in one station (station 5) is stable.

Acknowledgment

I would like to thank Dr. Erfan Omer Mossa for his assisting during the point load test performance. I also appreciate the assistance of Mr. Fahmy Osman Mohammed for supporting in drawing the location map by Arc-GIS software.

References

Abdullah, L. H. and Al-Qayim, B., 2016. GIS-based morphometric analysis of the Dewana basin, Sulaimani, Kurdistan, Iraq. JZS Journal, Special Issue, GeoKurdistan II Conference (163-187).

Azarafza M.; Asghari-Kaljahi E. and Akgün H., 2017. Assessment of discontinuous rock slope stability with block theory and numerical modeling: a case study for the South Pars Gas Complex, Assalouyeh, Iran. Environmental Earth Sciences, 76(11): 397.

Bar, N. and Barton, N., 2016. Empirical slope design for hard and soft rocks using Q-slope. In: Proceedings of the 50th US rock mechanics/ geomechanics symposium, ARMA 2016, Houston, 26–29 June 2016. ARMA 16-384.

Bar, N. and Barton, N., 2017. The Q-Slope Method for Rock Slope Engineering. Rock Mechanics and Rock Engineering, DOI: 10.1007/s00603-017-1305-0.

Barton, N.R.; Lien, R. and Lunde, J., 1974. Engineering classification of rock masses for the design of tunnel support. Rock Mechanics. Volume 6, pp. 189-236. Springer-Verlag.

Barton, N. R. and Bar, N., 2015. Introducing the Q-slope method and its intended use within civil and mining engineering projects. In: Proceedings of the ISRM Regional Symposium (Eurock 2015) and 64th Geomechaics Colloquium, Salzburg, Oct.

Barton, N.R. and Grimstad, E., 2014. An illustrated guide to the Q-system following 40 years use in tunnelling. In-house publisher: Oslo. Retrieved March 12, 2015 from www.nickbarton.com.

Bloom, A. L., 1998. Geomorphology – A systematic analysis of Late Cenozoic landforms (3rd edition). Prentice- Hall of India Private Limited, New Delhi, 482p.

Basahel, H. and Mitri, H., 2017. Application of rock mass classification systems to rock slope stability assessment: A case study. Journal of Rock Mechanics and Geotechnical Engineering, 9 (6): 993- 1009.

Bieniawski, Z.T., 1976. Rock mass classification in rock engineenig. In Exploration for rock engineering, Proc. of the Symp.,(ed. Z.T. Bieniawski). Vol.1, pp.97-106. Cape Town: Balkema.

Bieniawski, Z.T., 1989. Engineering rock mass classification. John Wiley, New York.

Bruce, I. G.; Cruden, D. M. and Eaton, T. M., 1989. Use of a tilting table to determine the basic friction angle of hard rock samples. Can. Geotech. J. 26, 274-279.

Gerrard, J., 1998. Rocks and landforms. Allen & Unwin Inc. Winchester, Mass. 319 pp.

Goodman, R. E., 1989. Introducion to rock mechanics 2nd edn., Wiley, New York, 562pp.

Hack, R.; Price, D. and Rengers, N., 2003. A new approach to rock slope stability–a probability classification (SSPC). Bull. Eng. Geol. Environ. 62, 167–184. https://doi.org/ 10.1007/s10064-002-0155-4.

Hamasur, G. A., 2013. Slope Stability Assessment Within and Around the Reservoir of the Proposed Basara Dam, Sulaimani, NE-Iraq. Iraqi Bulletin of Geology and Miming, Vol. 9, No. 3, pp: 51-66.

Hamasur, G. A. and Qadir, N. M., 2020. Slope Stability Assessment along Qalachwalan-Suraqalat Main Road, Sulaimani, NE-Iraq. Tikrit Journal of Pure Science, Vol. 25 (3).

Hocking, G., 1976. A method for distinguishing between single and double plane sliding of tetrahedral wedges. Int. J. Rock Mech. Min. Sci. Geomech. Abstr. 13, pp.225- 226.

Hoek, E. and Bray, J.W., 1981. Rock Slope Engineering. 3rd Edition, The Institution of Mining and Metallurgy, London, UK.

Huggett, J. R., 2011. Fundamentals of Geomorphology, 3rd ed., Routledge, New York. 516 pp.

Hussien, S. A.; Al-Kubaisi, M. Sh. and Hamasur, G. A., 2020. Impact of Geological Structures on Rock Slope Stability in The NW Nose (Plunge) of Surdash Anticline, Sulaimaniya/ NE Iraq. Iraqi Journal of Science, Vol. 61, No. 3, pp: 550-566.

ISRM, P.L.T., 1985. Suggested method for determining point load strength. Int J Rock Mech Min Sci Geomech Abstr, 22: 51–70.

Jackson, J. A.; Mehl, J. and Neuendorf, K., 2005. Glossary of Geology. American Geological Institute, Alexandria, Virginia. 800 pp.

Mamlesi, F. O., 2010. Engineering geological study of rock slope stability along Dokan-Khalakan road, Kurdistan region, NE-Iraq. Unpublished MSc thesis, University of Sulaimani, Iraq. 150 pp.

Markland, J.T., 1972. A useful technique for estimating the stability of rock slopes when the rigid wedge sliding type of failure is expected. Imp. Coll. Rock Mech. Res. Rep. 19, pp.10-26.

Palmstrom, A., 2005. Measurements of and correlations between block size and rock quality designation (RQD). Journal of Tunneling and Underground Space Technology, Vol.20 (4), pp.362–377.

Romana, M., 1985. New adjustment ratings for application of Bieniawski classification to slopes, in: Proceedings of the International Symposium on the Role of Rock Mechanics in Excavations for Mining and Civil Works. International Society of Rock Mechanics, Zacatecas, pp.49-53.

Rocscience: Inc. Dip v. 6.008, 2015. Graphical and statistical analysis of orientation data. Toronto, Canada.

Rusnak, J. and Mark, C., 2000. Using the point load test to determine the uniaxial compressive strength of coal measure rock. In: Proceedings of 19th international conference on ground control in mining, Morgantown, WV, pp.362–371.

Saranaathan, S. E. and Kannan, M., 2017. SMR and kinematic analysis for slope instability along Bodi-Bodimettu Ghat section, Tamil Nadu. Journal Geological Society of India, 89 (5): 589-599.

Sharma, M.; Sharma, S., Kumar, M. and Singh, S. K., 2019. Analysis of slope stability of road cut slopes of Srinagar, Uttakhand, India. International Journal of Applied Engineering Research ISSN 0973- 4562, 14 (3): 609-615.

Sullivan, T.D., 2013. Global slope performance index. Proceedings of Slope Stability, 55–80.

Twidale, C. R. and E.M. Campbell, E. M., 1993. Australian Landforms: Structure, Process and Time. Gleneagles Publishing, Adelaide, South Australia, Australia. 568 pp.